

Octahydrogenated Retinoic Acid-Conjugated Glycol Chitosan Nanoparticles as a Novel Carrier of Azadirachtin: Synthesis, Characterization, and *In Vitro* Evaluation

Wei Lu,^{1,2} Meng-Ling Lu,^{1,2} Qing-Peng Zhang,^{2,3} Yong-Qing Tian,^{1,2}
Zhi-Xiang Zhang,^{2,3} Han-Hong Xu^{1,2}

¹State Key Laboratory for Conservation and Utilization of Subtropical Agro-bioresources, South China Agricultural University, Guangzhou 510642, China

²Key Laboratory of Natural Pesticide and Chemical Biology of the Ministry of Education, South China Agricultural University, Guangzhou 510642, China

³Laboratory of Insect Toxicology, South China Agricultural University, Guangzhou 510642, China

Correspondence to: H. H. Xu (E-mail: hhxu@scau.edu.cn) or Z. X. Zhang (E-mail: zdsys@scau.edu.cn)

Received 2 May 2013; accepted 30 May 2013; published online 26 June 2013

DOI: 10.1002/pola.26801

ABSTRACT: Environment-friendly and controlled release formulation is highly promising for reducing environmental pollution and achieving the most effective utilization of pesticides. As a novel "green" nanocarrier of pesticides, amphiphilic self-assembled nanoparticles were prepared by chemical conjugation of octahydrogenated retinoic acid (OR) to the backbone of glycol chitosan (GC). In aqueous media, the synthesized OR-GC conjugates formed nanosized particles with a diameter of 257 nm. Hydrophobic azadirachtin (AZA) was efficiently loaded into the OR-GC nanoparticles at a feed weight ratio of up to 1:4 using a simple dialysis method, the maximum drug-loading efficiency of which was 74%. AZA-OR-GC (25 wt %) nanoparticles also showed sustained release of the

incorporated AZA (65% of the loaded dose was released in 7 days at 27 °C in phosphate-buffered saline; pH 7.2). Cytotoxicity tests and cell cycle arrest assays confirmed that OR-GC exhibits good biocompatibility; AZA-OR-GC (25 wt %) nanoparticles also showed favorable inhibition of cell proliferation in SI-1 cells compared with free AZA in organic solvents. Overall, controlled release AZA-OR-GC may be a promising environment-friendly formulation for integrated pest management. © 2013 Wiley Periodicals, Inc. *J. Polym. Sci., Part A: Polym. Chem.* **2013**, *51*, 3932–3940

KEYWORDS: azadirachtin; glycol chitosan; *in vitro* evaluation; nanocarrier; self-assembled nanoparticles; SI-1 cells

INTRODUCTION Azadirachtin (AZA) is a potent tetranortriterpenoid botanical insecticide extracted from the seeds of neem tree (*Azadirachta indica*). It has demonstrated significant advantages in integrated pest management (IPM) against a wide range of insect pests, such as a broad spectrum of activity, no known insecticide resistance mechanisms, new mode of action with possible multiple sites of attack, compatibility with many commercial insecticides, fungicides, and other biological agents, and minimal impact on nontarget organisms.^{1–4} AZA is a hydrophobic pesticide with low water solubility (0.26 mg mL⁻¹, 20 °C).^{5,6} Sunlight or UV can quickly degrade AZA because its molecules contain unstable groups, such as olefinic bond, epoxy, and enol structures.^{7,8} However, traditional formulations of emulsifiable AZA concentrates and dusts employ a large amount of organic reagents, which are not conducive to reducing environmental pollution, promoting food safety and human

health. Therefore, the development of pesticide formulations has paid significant attention to environmental safety, reductions in organic solvent usage, and improving the bioavailability and persistence of the active ingredient.⁹ Many studies have focused on developing novel environment-friendly and controlled release aqueous solutions.¹⁰

Nanosized drug carriers, such as micelles, nanoparticles, polymer-drug conjugates, and stealth liposomes, have been investigated in attempts to enhance drug efficacy and bioavailability.^{11,12} Polymeric amphiphiles consisting of hydrophilic and hydrophobic segments have received much attention because they can form self-assembled nanoparticles and exhibit good physicochemical and controlled release characteristics. In the aqueous phase, the hydrophobic cores of polymeric nanoparticles are surrounded by hydrophilic outer shells. Thus, self-assembled polymeric nanoparticles

Additional Supporting Information may be found in the online version of this article.

© 2013 Wiley Periodicals, Inc.

have been recognized as promising drug carriers because their inner core can serve as reservoirs for hydrophobic drugs.^{13,14}

Significant research attention has recently been paid to the preparation of biodegradable and nontoxic polymeric amphiphiles based on natural biomaterials, such as chitosan.⁹ Chitosan and its derivatives have specific structures and physicochemical properties, leading to excellent biocompatibility, biodegradability, low immunogenicity, and biological activities.^{15–17} However, chitosan is soluble only in acidic aqueous solutions below pH 6.5.¹⁸ Most chitosan-based self-aggregates precipitate within a few days in biological solution (pH 7.4), which restricts the medical application of chitosan and its derivatives in drug delivery systems.¹⁹ However, glycol chitosan (GC) is a novel chitosan derivative and carrier of drugs because of its solubility in water at all pH values and biocompatibility.²⁰ Many studies have focused on hydrophobically modified GC derivatives, such as GC-5- β -cholic acid, GC-deoxycholic acid, GC-*N*-acetyl histidine, GC-cholesterol, GC-hydrotropic oligomer, GC-protoporphyrin, GC-tocol, and GC-ergocalciferol succinate conjugates, because of their amphiphilic structure.^{14,21–28} These polymeric amphiphiles can form monodispersed self-aggregated nanoparticles in aqueous media and show good stable nanoparticle structures in physiological conditions. Many investigations have confirmed that these nanoparticles can be used as carriers for hydrophobic medicines, gene delivery, and medical diagnosis.^{29–36}

Few nanoparticle carriers for pesticides are available. *In vitro* evaluation of GC-based nanoparticles for pesticide delivery has yet to be reported. Therefore, we attempted to prepare octahydrogenated retinoic acid (OR)-conjugated GC (OR-GC) nanoparticles as a novel environment-friendly carrier that can contain AZA in aqueous media. To produce AZA-loaded OR-GC (AZA-OR-GC) nanoparticles, we encapsulated AZA into the OR-GC nanoparticles by a simple dialysis method. To evaluate the characteristics of AZA-OR-GC *in vitro*, its drug release profile, cytotoxicity, and cell cycle analysis were studied in comparison with those of free AZA.

EXPERIMENTAL

Materials

GC ($M_w = 5.3 \times 10^5$, degree of deacetylation = 91%) was purchased from Sigma-Aldrich Trading. All-trans retinoic acid was purchased from Yuancheng Gongchuang Technology. AZA (purity 45%, the experiments mentioned AZA weight are the weight of the active ingredient) was produced by the Key Laboratory of Pesticide and Chemical Biology of the Ministry of Education, South China Agricultural University, China. 1-Ethyl-3-(3-dimethylaminopropyl)-carbodiimide hydrochloride (EDC) and *N*-hydroxysuccinimide (NHS) were purchased from Aladdin Chemistry. Methanol and anhydrous dimethyl sulfoxide (DMSO) were purchased from Dikma Technologies. Pure water used in all the experiments was obtained by ELGA Pure Lab-ultra water purification system (resistance

>10 M Ω). All other chemicals were purchased from Sino-pharm Chemical Reagent, which were analytical grade and used without further purification.

Synthesis of Octahydrogenated Retinoic Acid

A suspension of retinoic acid and 10% palladium on carbon in anhydrous cyclohexane/ethanol (1:1 v/v) was stirred in reactor under H₂ (4.04×10^5 Pa) for 24 h. The reaction mixture was filtered through a pad of Celite. The filtrate was concentrated under reduced pressure and the residue was purified by silica gel column chromatography (petroleum ether/ethyl acetate, 13:1 v/v) to afford OR as pale yellow oil.

¹H NMR (600 MHz, CD₃OD, δ): 2.28 (dd, $J = 1.2, 6.0$ Hz, 1H; CH₂), 2.25 (dd, $J = 1.2, 5.4$ Hz, 1H; CH₂), 2.10 (dt, $J = 1.8, 7.8$ Hz, 1H; CH₂), 2.07 (dt, $J = 1.8, 7.8$ Hz, 1H; CH₂), 1.93 (t, $J = 6.0$ Hz, 2H; CH₂), 1.60 (s, 3H; CH₃). ¹³C NMR (150 MHz, CD₃OD, δ): 177.1 (C=O), 138.7 (C6), 127.4 (C5), 42.7 (C14), 41.1 (C2), 38.3 (C8), 38.1 (C9), 35.9 (C10), 35.2 (C1), 33.8 (C4), 31.4 (C13), 27.9 (C16), 27.9 (C17), 23.6 (C11), 23.6 (C7), 20.2 (C19), 20.1 (C3), 20.1 (C18), 20.1 (C20).

Preparation of OR-GC Nanoparticles

OR-GC conjugates were prepared by conjugation of GC with OR in the presence of NHS and EDC, which produces amide linkages between the amine groups of GC and carboxyl acid groups of retinoic acid, as previously reported for other amphiphilic polymers.³⁷ GC was purified by filtration and dialyzed against pure water for three times. The purified GC (100 mg, 0.189 μ mol) was dissolved in pure water (10 mL), and OR (60 mg, 195 μ mol) dissolved in methanol (10 mL) was added under vigorous stirring. The chemical modification was initiated by adding equal amounts (1.5 equiv/OR) of NHS and EDC. Thereafter, the reaction was allowed to proceed for 24 h at room temperature. The solution was dialyzed using dialysis tube (M_w cutoff = 12,000–14,000) for 3 days with 12 exchanges to remove unreacted chemicals. The dialysis was performed by three steps [water/methanol (1:4 v/v), water/methanol (1:1 v/v), and pure water at days 1, 2, and 3, respectively]. Finally, the dialyzed solution was lyophilized for 2 days to produce a white, cotton wool-like product. The chemical structure of OR-GC conjugates was analyzed using ¹H NMR spectra in CD₃OD/D₂O (3:1 v/v) at 600 MHz (Bruker). FTIR spectra were recorded on Fourier-transform infrared spectrometer (Nicolet 6700, Thermo Fisher Scientific, USA) in KBr discs. The degree of substitution (DS) defined as the number of OR per 100 sugar residues of GC was determined by ¹H NMR.

Critical Micelle Concentration

The critical micelle concentration (CMC) of OR-GC was determined using the fluorescence probe method.⁹ Briefly, a known amount of pyrene in tetrahydrofuran was added to each of a series of 10-mL vials and the tetrahydrofuran was evaporated at room temperature. The polymer concentration varied from 10^{-5} to 1 mg mL⁻¹, the final concentration of pyrene was set to 6×10^{-7} M for all samples, and then sonicated for 30 min. The sample solutions were heated at

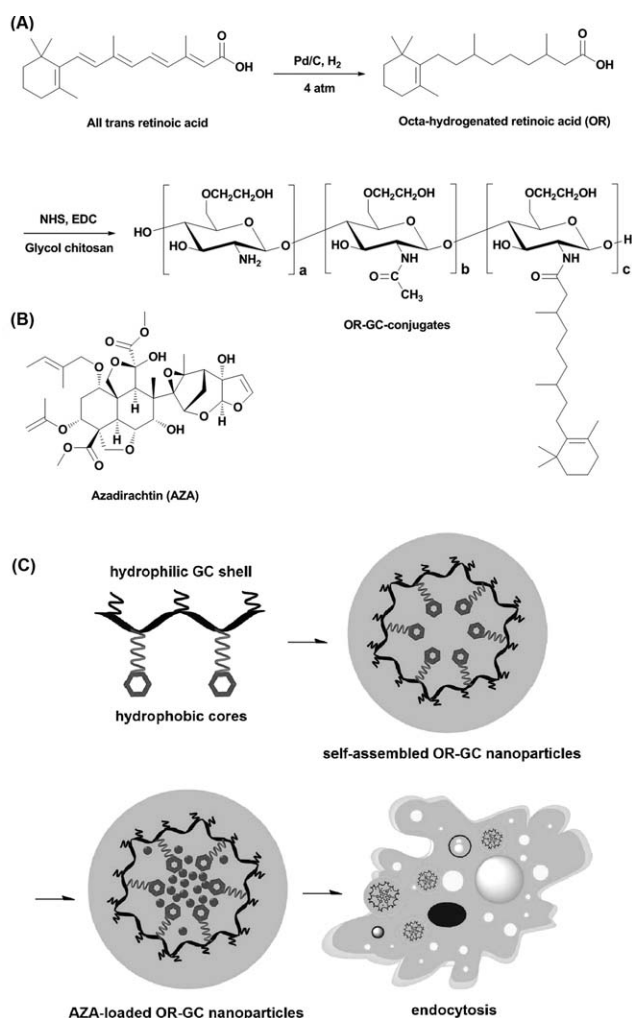


FIGURE 1 Schematic representation of the synthetic route for the glycol chitosan-octahydrogenated retinoic acid (OR-GC) conjugates (A) and chemical structure of azadirachtin (B). Schematic diagram of AZA-loaded OR-GC nanoparticles (C).

40 °C for 3 h to equilibrate the pyrene and the nanoparticles and left to cool overnight at room temperature. Fluorescence spectra were measured at the excitation wavelength (λ_{ex}) of 355 nm with a Hitachi F-4600 Fluorescence spectrophotometer (Japan). Both excitation and emission bandwidth were set at 2.5 nm, and the emission wavelength was 350–450 nm for emission spectra.

Preparation of AZA-Loaded OR-GC (AZA-OR-GC) Nanoparticles

AZA-OR-GC nanoparticles were prepared by the dialysis method. The synthesized OR-GC conjugates (100 mg) were dissolved in 10 mL of water/methanol (1:1 v/v) and AZA (25–100 mg) in 2 mL of methanol was added to the OR-GC solution. The solution was vigorously stirred for 12 h at room temperature and then dialyzed against pure water using dialysis tube (M_w cutoff = 12,000–14,000). After dialysis for 2 days, the solution was centrifuged at 10,000g for 30 min to remove the unloaded AZA. The supernatant was

filtered through a 0.8- μ m membrane filter and then lyophilized to give a pale yellow powder. The drug loading efficiency of AZA-OR-GC nanoparticles was measured by high-performance liquid chromatography (Agilent 1100 series). The samples were analyzed for the AZA concentration by reverse-phase HPLC system with Agilent TC C₁₈ column (4.6 mm \times 250 mm) at a constant temperature of 30 °C. The mobile phase consisted of 65:35 (v/v) methanol/water and was delivered at a flow rate of 1.0 mL min⁻¹. Eluted compounds were detected at 218 nm using diode array detector.

Characterization of AZA-OR-GC Nanoparticles

The mean diameter and ζ -potential of OR-GC and AZA-OR-GC nanoparticles were measured by dynamic light scattering (DLS) using Malvern Zetasizer 90 (Malvern Instruments, England). The sample concentration was kept at 1.667 mg mL⁻¹ in pure water. The morphology of nanoparticles was observed by transmission electron microscopy (TEM) (Tecnai G² Spirit, FEI, Netherlands), operated at an acceleration voltage of 120 kV. Each sample (2 mg mL⁻¹ in pure water) was placed on a 300-mesh copper grid coated with carbon. Subsequently, the sample was dried and negatively stained using 2% phosphotungstic acid dye solution.

In Vitro AZA Release Profile of AZA-OR-GC Nanoparticles

To determine the *in vitro* release profile of AZA from OR-GC nanoparticles, lyophilized AZA-OR-GC nanoparticles (8 mg) were dispersed in 2 mL of phosphate-buffered saline (PBS) (pH 7.2). The resulting solution was placed into a cellulose membrane dialysis tube (M_w cutoff = 12,000–14,000). The dialysis tube was placed in 30 mL of PBS buffer and gently shaken at 27 °C in water bath at 100 rpm. At various time points, the medium was refreshed. The concentration of AZA was determined by UV-vis spectroscopy (Shimadzu, Japan).

Cytotoxicity of AZA-OR-GC Nanoparticles

Spodoptera litura cultured ovarian cell lines SI-1 obtained from Sun Yat-sen University, College of Life Sciences (Guangzhou, China) were routinely cultured in antibiotic-free Grace's medium containing 7% fetal bovine serum, 0.3% yeast extract, and 0.3% lactalbumin hydrolysate. The cytotoxicity of OR-GC, free AZA, and AZA-OR-GC nanoparticles was evaluated by the MTT assay. Cells were seeded at a density of 2×10^4 cells per well in 96-well flat-bottomed plates, allowed to adhere for overnight, and incubated for 24 h at 27 °C in 0.4% CO₂. Five milligrams of AZA dissolved in 1 mL of DMSO was prepared for AZA stock solution, followed by sonication for 5 min. The stock solutions of AZA-OR-GC nanoparticles in PBS (pH 7.2) were prepared by mixing 26.7 mg of OR-GC and 6.7 mg AZA by a dialysis method. Each stock solution was diluted with culture medium to obtain a concentration in the range of 0.5–50 μ g mL⁻¹. DMSO (0.1%) was used as the control and empty OR-GC also tested as vehicle controls for the same concentrations. After 24, 48, 72, and 96 h of treatment, 10 μ L MTT (5 mg mL⁻¹) was added to each well and the cells were incubated further for 4 h at 27 °C. The medium was removed and each well was

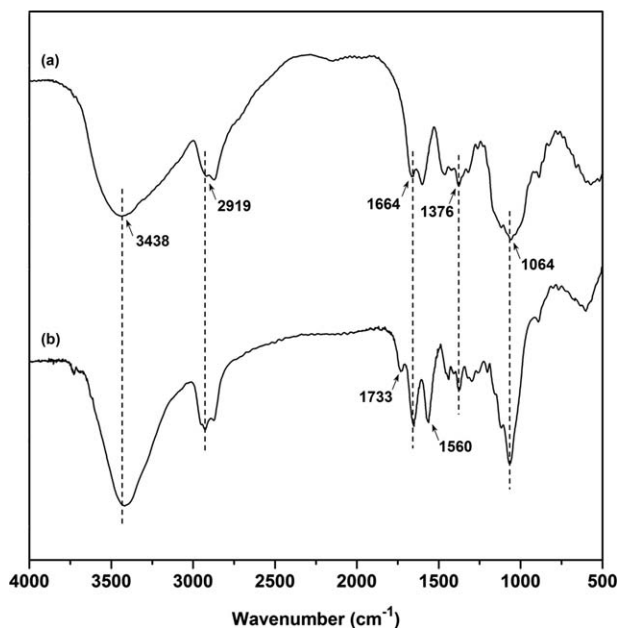


FIGURE 2 FTIR spectra of GC (a) and OR-GC (b).

added 100 μL of DMSO. The absorbance was measured at 570 nm by a microplate reader (Bio-Rad, USA).³⁸

Cell Cycle Analysis by Flow Cytometry

Cells were plated in plastic culture dishes and cultured at 27 °C in 0.4% CO_2 . When the density was 10^6 cells mL^{-1} ,

cells were incubated with OR-GC, AZA, and AZA-OR-GC at 27 °C for serial times (24, 48, 72, and 96 h). After harvested, cells were washed three times with 1 mL of PBS (pH 7.2) and fixed in ice-cold 70% ethanol. After refrigerated overnight at 4 °C, the cells were washed with PBS to remove residual ethanol and resuspended in propidium iodide stain buffer for 30 min at 27 °C. The cell cycle phases of the total cell population (G0/G1, S, and G2/M) were analyzed using Becton Dickinson flow cytometer (USA).

RESULTS AND DISCUSSION

Preparation of OR-GC Nanoparticles

OR-GC is an amphiphilic polymer consisting of hydrophilic and hydrophobic segments. In the aqueous phase, OR serves as a hydrophobic core of polymers surrounded by hydrophilic outer shells. Thus, the inner core can serve as a nanocontainer for hydrophobic pesticides. As a nanosized pesticide carrier, biocompatible and biodegradable GC was hydrophobically modified by OR in the presence of NHS and EDC [Fig. 1(A)]. Formation of the amide linkage between GC and OR was demonstrated by the FTIR and ^1H NMR spectra.

Figure 2 shows the FTIR spectra of GC and OR-GC. The absorption peaks of GC are as follows: 3438 cm^{-1} ($\nu_{\text{O-H}}$ overlapped with $\nu_{\text{N-H}}$), 2919 and 2873 cm^{-1} (aliphatic $\nu_{\text{C-H}}$), 1664 cm^{-1} (amide I band, $\nu_{\text{C=O}}$ of acetyl group), 1600 cm^{-1} ($\nu_{\text{N-H}}$), 1461 – 1376 cm^{-1} ($\nu_{\text{C-H}}$), and 1064 cm^{-1} (skeletal vibrations involving the $\nu_{\text{C=O}}$). Compared with that of GC, the spectrum of OR-GC showed an intense peak at

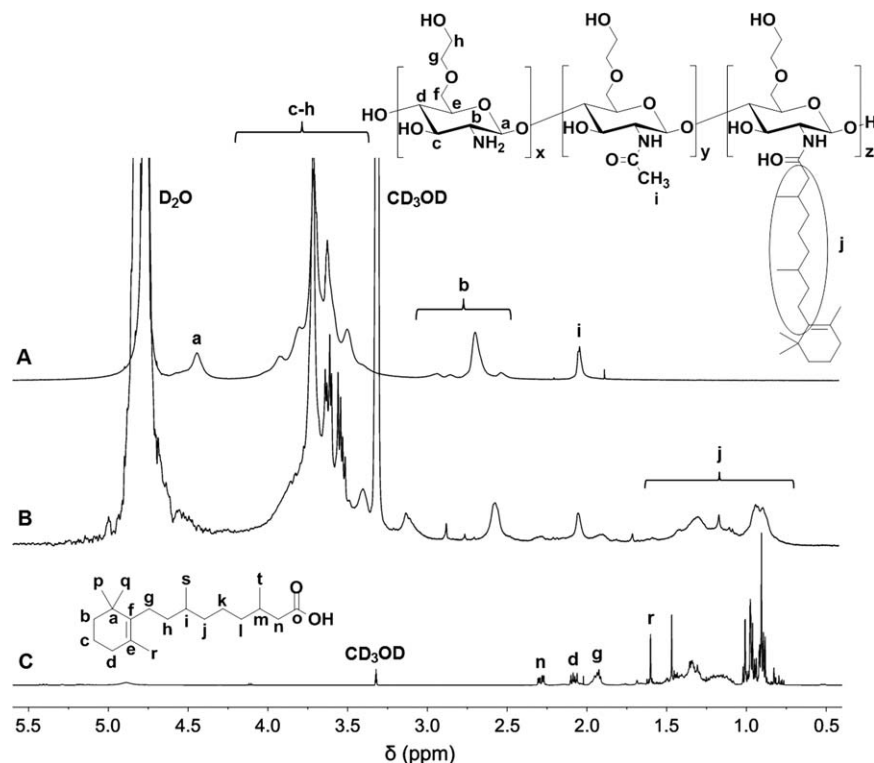


FIGURE 3 ^1H NMR spectra of GC in D_2O (concentration = 25 mg mL^{-1}) (a), OR-GC in $\text{CD}_3\text{OD}/\text{D}_2\text{O}$ (3:1 v/v) (concentration = 20 mg mL^{-1}) (b), and OR in CD_3OD (concentration = 20 mg mL^{-1}) (c).

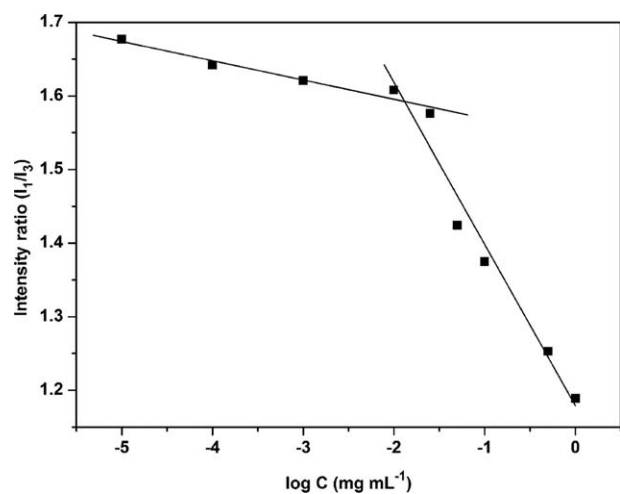


FIGURE 4 Plot of the intensity ratio I_1/I_3 (from pyrene excitation spectra) as a function of $\log C$.

1560 cm^{-1} (amide II band, $\nu_{\text{N-H}}$), an increased peak at 1733 cm^{-1} assigned to the $\nu_{\text{C=O}}$ of amide bond in synthesized OR-GC conjugate, and an increase in the amide I bending peak at 1650 cm^{-1} , which confirmed the amide linkage between GC and OR.

^1H NMR spectrum and results are shown in Figure 3. The proton signals of GC are as follow: 1.98 ppm (CH_3 , methyl protons of the acetyl group of *N*-acetamidoglucose units), 2.63 ppm (CH, C_b sugar protons of the *N*-substituted glucosamine units), 3.04–4.16 ppm (CH, C_c to C_h sugar protons), and 4.38 ppm (CH, C_a anomeric sugar proton).^{14,28} Compared with those of GC, the proton signals of OR-GC showed peaks at 0.60–1.60 ppm, belonging to the high field signals of OR. These results indicate that the OR group had been incorporated into the GC. The DS, defined as the number of OR molecules per 100 sugar residues of GC, was 20.4. On average, OR-GC conjugates had 351 molecules of OR in one GC polymer.

Critical Micelle Concentration

The CMC of OR-GC was determined using the fluorescence probe method. Pyrene molecules are reported to preferably localize inside or close to the hydrophobic microenvironment of micelles, varying with different molecular photophysical properties.¹⁴ The emission intensity ratio of the first (372 nm, I_1) and third (382 nm, I_3) peaks is used to monitor

the aggregation behavior of surfactants or polymers in polar solutions. When the concentration of OR-GC was increased, the intensity ratio (I_1/I_3) decreased significantly with the transfer of pyrene from an aqueous polar environment to a more hydrophobic medium. The CMC of OR-GC was determined to be $13\ \mu\text{g mL}^{-1}$ (Fig. 4). These results suggest that the micelle core was very hydrophobic.

Preparation of AZA-OR-GC Nanoparticles

AZA-OR-GC nanoparticles were simply prepared using a dialysis method and the overall characteristics of the products are summarized in Table 1. In aqueous environments, the hydrophilic GC is situated outside of the molecules because of hydrophilic interactions with water and the insoluble AZA is found inside the molecules because of their hydrophobic intermolecular and intramolecular interactions.^{22,28} To determine the loading capacity, we varied the feed weight ratio of AZA from 25 to 100 wt % and found that the loading efficiency of AZA into OR-GC nanoparticles decreased with increasing amount of loaded AZA. When the AZA content in OR-GC was 25 wt %, the maximum loading efficiency of AZA-OR-GC nanoparticles was about 74%, which is attributed to the presence of hydrophobic inner cores. An important observation is that the AZA-OR-GC nanoparticles were well dispersed in aqueous medium. However, when the feed amount of AZA was increased to above 100 wt %, the excess AZA molecules precipitated during dialysis and the loading efficiency significantly decreased to about 43%.

Based on the results of DLS analysis, the average diameter of AZA-OR-GC increased with increasing loading content. These observations show that AZA molecules are wrapped in the hydrophobic inner cores of OR-GC and that entrapped AZA molecules cause an increase in the mean diameter of the OR-GC nanoparticles. The AZA-OR-GC nanoparticles spontaneously self-aggregated to spheroids with an average diameter of 312–410 nm in aqueous conditions, as determined by DLS and TEM (Fig. 5). With the aim of achieving higher loading efficiency, we optimized the feed ratio of AZA into OR-GC to 25 wt %. Figure 5 displays the diameters of the OR-GC and AZA-OR-GC (25 wt %) nanoparticles, which were almost spherical and well-dispersed without aggregation.

In Vitro Release Profile of AZA-OR-GC Nanoparticles

To improve the efficacy of AZA, sustained release of AZA from polymeric nanoparticles was studied. To evaluate the potential of OR-GC nanoparticles as a pesticide carrier of

TABLE 1 Physical Characteristics of AZA-Loaded OR-GC Nanoparticles

Sample	Loading Content of AZA (wt %)	Loading Efficiency (%)	Diameter (nm)	ζ -Potential (mV)
OR-GC	–	–	257 ± 12	38.1 ± 0.8
AZA-OR-GC (25 wt %)	18.4 ± 0.5	73.6 ± 1.9	312 ± 16	28.3 ± 0.5
AZA-OR-GC (50 wt %)	31.1 ± 0.7	62.2 ± 1.3	379 ± 18	21.2 ± 0.3
AZA-OR-GC (100 wt %)	42.7 ± 2.4	42.7 ± 2.4	410 ± 10	25.3 ± 0.3

Mean diameter in pure water as measured by dynamic light scattering ($n=3$). The OR-GC and AZA-OR-GC nanoparticles concentrations are 1.667 mg mL^{-1} .

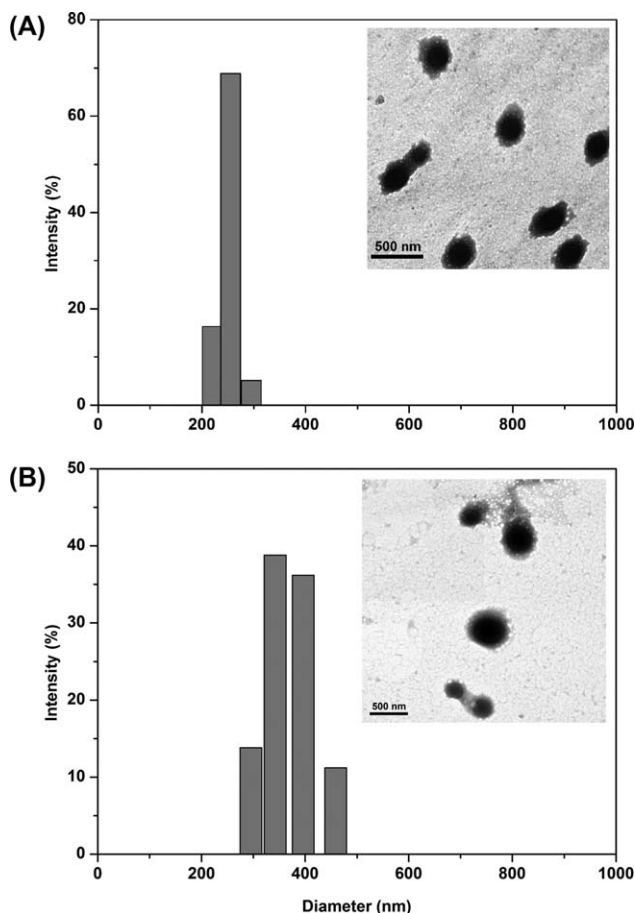


FIGURE 5 Particle size and morphological shapes of OR-GC (A) and AZA-OR-GC nanoparticles (B). Average size of OR-GC and AZA-OR-GC (25 wt %) nanoparticles (1.667 mg mL^{-1} in pure water) was measured using dynamic light scattering. Inset image indicated TEM image of OR-GC and AZA-OR-GC (25 wt %) nanoparticles in pure water (2 mg mL^{-1}).

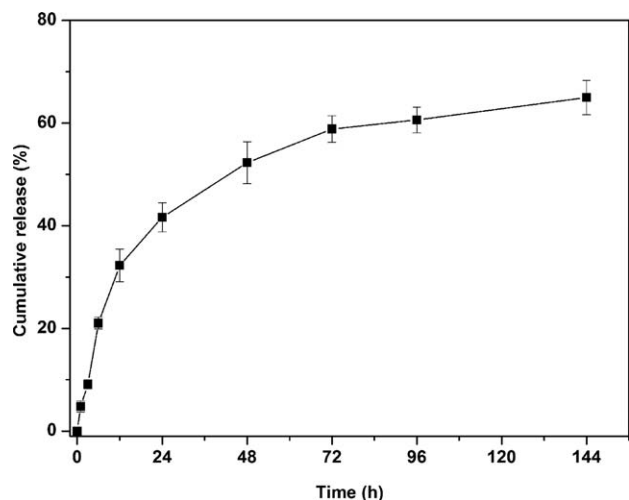


FIGURE 6 AZA release profile from nanoparticles at $27 \text{ }^\circ\text{C}$ in PBS ($\text{pH} = 7.2$). Data represent mean \pm SD ($n = 3$).

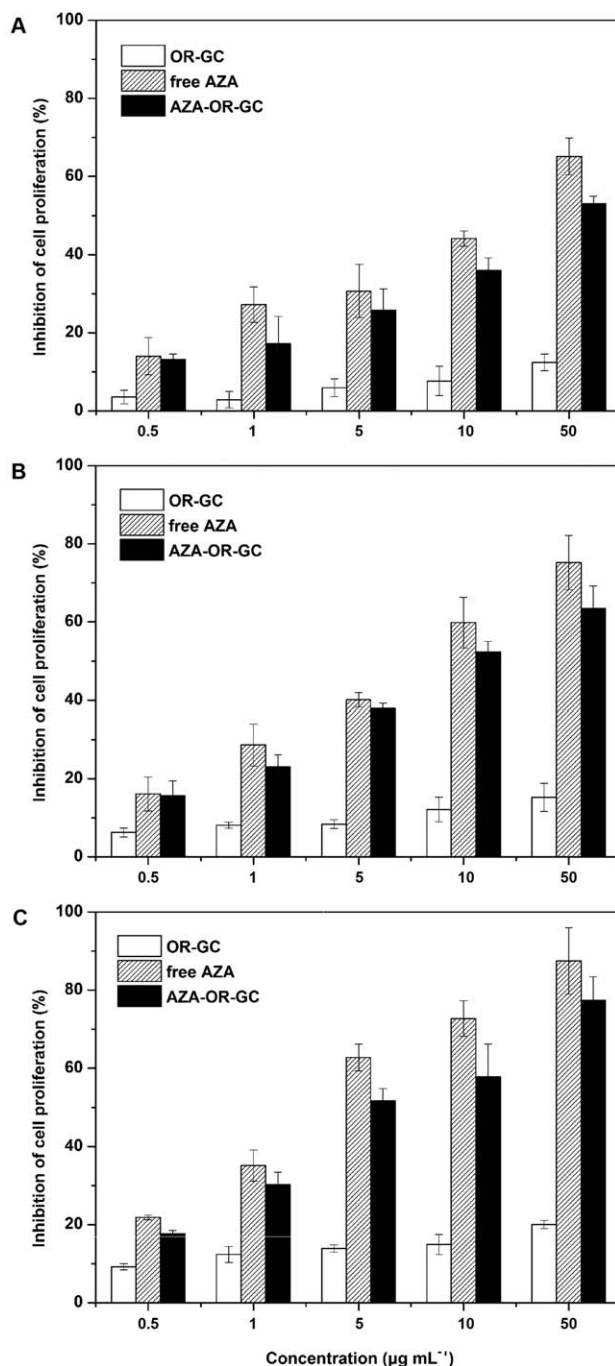


FIGURE 7 Cytotoxicity of AZA-OR-GC (25 wt %) nanoparticles. Inhibition of cell proliferation of each sample was measured using MTT assay after treated for 48 h (A), 72 h (B), and 96 h (C). Data represent mean \pm SD ($n = 3$).

AZA, the release behavior of AZA from OR-GC nanoparticles was assessed at $27 \text{ }^\circ\text{C}$ in PBS ($\text{pH} 7.2$). During this test, the sink conditions were maintained by regularly replacing the dialysis medium. Figure 6 shows the *in vitro* AZA release profile from AZA-OR-GC (25 wt %) nanoparticles. An initial rapid release phase burst effect was observed within 12 h, and 30% of the AZA was released from the nanoparticles. After the first 12 h, the cumulative release of AZA gradually

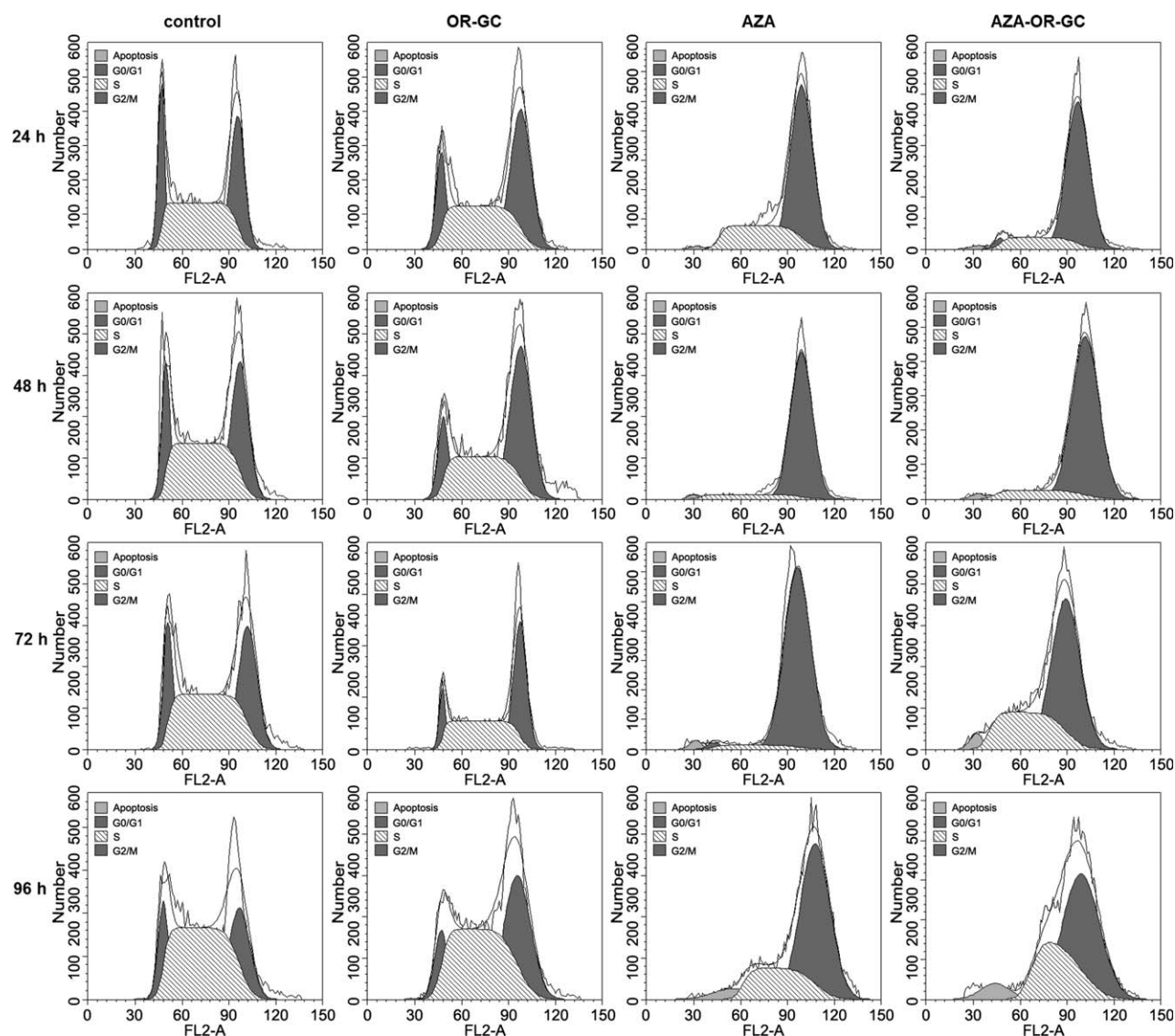


FIGURE 8 Cell cycle distribution of SI-1 cells. Cells were incubated in OR, AZA, and AZA-OR-GC (25 wt %) for 24, 48, 72, and 96 h, and analyzed by flow cytometry. The equivalent AZA concentration was $10 \mu\text{g mL}^{-1}$.

plateaued and release was sustained for the following 6 days. Approximately 65% of the AZA was released over 7 days, indicating the potential application of the nanoparticles in sustained pesticide delivery systems. These two phases may be controlled by a diffusion mechanism resulting from partitioning between polymer nanoparticles and the surrounding aqueous phase. The initial rapid release phase may be due to weak interactions between the released AZA molecules and the hydrophobic moiety of nanoparticles, and the subsequent sustained release phase may be due to strong interactions between the released AZA molecules and the hydrophobic nanoparticles cores.²⁸

Cytotoxicity of AZA-OR-GC Nanoparticles in SI-1 Cells

Pesticide delivery carriers must be biocompatible and environment-friendly for their successful utilization in the field of agricultural chemicals. Thus, the cytotoxicity of free

AZA dissolved in DMSO and AZA-OR-GC (25 wt %) nanoparticles in PBS was evaluated by determining their inhibitory effects on SI-1 ovarian cell proliferation (Fig. 6). Based on the MTT test, empty OR-GC nanoparticles as a vector control showed slight cytotoxicity varying from 0.5 to $50 \mu\text{g mL}^{-1}$. By contrast, all of the samples exhibited significant cytotoxicity against the SI-1 cells, which was further enhanced by increasing the time of exposure and AZA concentration. When the SI-1 cells were treated with $50 \mu\text{g mL}^{-1}$ for 48 h, inhibition of cell proliferation by AZA-OR-GC (25 wt %) was 53% compared with that by free AZA (65%). After 96 h of treatment, inhibition of cell proliferation of AZA-OR-GC (25 wt %) nanoparticles increased to 77% compared with that by free AZA (87%) at $50 \mu\text{g mL}^{-1}$. These results show that the cytotoxicity of AZA-OR-GC (25 wt %) against SI-1 cells is relatively lower than that of DMSO-based AZA, which may be attributed to the slow and sustained release of AZA

TABLE 2 Cell Cycle Distribution (20,000 Cells Per Count)

Treatment	Cell Cycle Distribution (%)				
	Apoptosis	G0/G1	S	G2/M	
24 h	Control	0.0	20.0	48.1	32.0
	OR-GC	0.0	15.2	41.3	43.6
	AZA	0.7	0.1	29.3	70.6
	AZA-OR-GC	1.2	2.9	17.0	80.1
48 h	Control	0.0	17.3	48.1	34.6
	OR-GC	0.0	13.1	38.7	48.2
	AZA	1.5	0.0	10.5	89.5
	AZA-OR-GC	1.1	0.0	12.1	87.9
72 h	Control	0.0	17.2	49.6	33.2
	OR-GC	0.0	10.8	45.2	43.4
	AZA	2.0	1.7	5.6	92.7
	AZA-OR-GC	3.0	0.0	34.4	65.6
96 h	Control	0.1	14.2	59.6	26.2
	OR-GC	0.1	10.8	50.5	38.7
	AZA	6.2	0.1	28.0	72.0
	AZA-OR-GC	6.1	0.1	34.1	65.8

molecules from OR-GC nanoparticles. The OR-GC nanoparticles maintained the toxicological activity of AZA and efficiently delivered it to the cells. Therefore, the OR-GC nanoparticle-based formulation showed high antiproliferative activities in SI-1 cells (Fig. 7).

Effect of Nanoparticles on Cell Cycles Arrest

Flow cytometry was used to analyze the influence of AZA and AZA-OR-GC nanoparticles on the cell cycle (Fig. 8). Based on the cell cycles arrest test, the cell cycle distribution of OR-GC nanoparticles did not change significantly compared with the control. Upon treatment with $10 \mu\text{g mL}^{-1}$ for 24 h, the percentage of AZA- and AZA-OR-GC- (25 wt %) treated cells in the G2/M phase increased to more than 71% compared with that of control cells (32%) and began to appear apoptosis. After 96 h of treatment, apoptosis rate of AZA and AZA-OR-GC was 6.2 and 6.1%, respectively. Subsequent AZA release from AZA-OR-GC nanoparticles into the cytosol caused cell cycle arrest in the G2/M phase, differing markedly from observations of control cells. These results indicate that AZA-OR-GC nanoparticles can sustain the release of AZA molecules and inhibit SI-1 cell proliferation, consistent with the results of the MTT test (Table 2).

CONCLUSIONS

We have explored a novel amphiphilic OR-GC conjugate for preparing “green” AZA nanoparticles, which can self-assemble with approximately spherical morphology in pure water. The most significant feature of the proposed nanoparticle system is its amphiphilic core-shell structure, which can effectively to load the poorly water-soluble pesticide AZA (about 74%). AZA-OR-GC nanoparticles were observed a

controlled release, achieving roughly a 65% of loaded drug in 7 days in PBS (pH 7.2). Compared with free AZA in organic solvents, the AZA-OR-GC nanoparticles showed favorable inhibition of cell proliferation and sustained drug release performance in SI-1 cells *in vitro*. Finally, environment-friendly and controlled release AZA-encapsulated OR-GC formulations showed great potential to apply in IPM.

ACKNOWLEDGMENTS

This research was financially supported by Agro-scientific Research in the Public Interest of China (No. 200903052) and Science and Technology Planning Project of Guangdong Province, China (No. 2012B020309004). The authors thank Zhuo-Qiang Zhou (College of Science, South China Agricultural University) for the synthesis of OR, and Zhi-Wei Lei for NMR spectrum analysis.

REFERENCES AND NOTES

- 1 E. D. Morgan, *Bioorg. Med. Chem.* **2009**, *17*, 4096–4105.
- 2 Y. Liu, G. S. Chen, Y. Chen, J. Lin, *Bioorg. Med. Chem.* **2005**, *13*, 4037–4042.
- 3 X. Y. Huang, W. O. Li, H. H. Xu, *Pestic. Biochem. Physiol.* **2010**, *98*, 289–295.
- 4 C. Yan, Z. X. Zhi, H. Xu, *J. Biotechnol.* **2012**, *159*, 115–120.
- 5 International Union of Pure & Applied Chemistry, Pesticide Properties Database. *Azadirachtin*, Ref: N3101. Available at: <http://sitem.herts.ac.uk/aeru/iupac/> (Accessed 4/6/2011).
- 6 P. Jarvis, S. Johnson, E. D. Morgan, *J. Pestic. Sci.* **1998**, *53*, 217–222.
- 7 P. T. Deota, P. R. Upadhyay, V. B. Valodkar, *Nat. Prod. Res.* **2003**, *17*, 21–26.
- 8 S. Johnson, P. Dureja, S. Dhingra, *J. Environ. Sci. Health B* **2003**, *38*, 451–462.
- 9 S.B. Lao, Z. X. Zhang, H. H. Xu, G. B. Jiang, *Carbohydr. Polym.* **2010**, *82*, 1136–1142.
- 10 S. He, W. Zhang, D. Li, P. Li, Y. Zhu, M. Ao, J. Li, Y. Cao, *J. Mater. Chem. B* **2013**, *1*, 1270–1278.
- 11 J. H. Kim, Y. S. Kim, K. Park, S. Lee, H. Y. Nam, K. H. Min, H. G. Jo, J. H. Park, K. Choi, S. Y. Jeong, R. W. Park, I. S. Kim, K. Kim, I. C. Kwon, *J. Control. Release* **2008**, *127*, 41–49.
- 12 J. H. Na, S. Y. Lee, S. M. Lee, H. B. Koo, K. H. Min, S. Y. Jeong, S. H. Yuk, K. Kim, I. C. Kwon, *J. Control. Release* **2012**, *163*, 2–9.
- 13 J. H. Kim, Y. S. Kim, S. Kim, J. H. Park, K. Kim, K. Choi, H. Chung, S. Y. Jeong, R. W. Park, I. S. Kim, I. C. Kwon, *J. Control. Release* **2006**, *111*, 228–234.
- 14 J. M. Yu, Y. J. Li, L. Y. Qiu, Y. Jin, *Eur. Polym. J.* **2008**, *44*, 555–565.
- 15 J. H. Park, Y. W. Cho, H. Chung, I. C. Kwon, S. Y. Jeong, *Biomacromolecules* **2003**, *4*, 1087–1091.
- 16 S. He, W. Zhang, D. Li, P. Li, Y. Zhu, M. Ao, J. Li, Y. Cao, *J. Mater. Chem.* **2013**, *9*, 1270–1278.
- 17 M. N. Kumar, R. A. Muzzarelli, C. Muzzarelli, H. Sashiwa, A. J. Domb, *Chem. Rev.* **2004**, *104*, 6017–6084.
- 18 J. H. Park, S. Kwon, M. Lee, H. Chung, J. H. Kim, Y. S. Kim, R. W. Park, I. S. Kim, I. S. Kim, S. B. Seo, I. C. Kwon, S. Y. Jeong, *Biomaterials* **2006**, *27*, 119–126.

- 19 E. A. Stepnova, V. E. Tikhonov, T. A. Babushkina, T. P. Klimova, E. V. Vorontsov, V. G. Babak, S. A. Lopatin, I. A. Yamskov, *Eur. Polym. J.* **2007**, *43*, 2414–2421.
- 20 F. Uchegbu, L. Sadiq, M. Arastoo, A. I. Gray, W. Wang, R. D. Waigh, A. G. Schätzlein, *Int. J. Pharm.* **2001**, *224*, 185–199.
- 21 H. Park, S. Kwom, J. O. Nam, R. W. Park, H. Chung, S.B. Seo, I. S. Kim, I. C. Kwon, S. Y. Jeong, *J. Control. Release* **2004**, *95*, 579–588.
- 22 H. Kim, Y. S. Kim, S. Kim, J. H. Park, K. Kim, K. Choi, H. Chung, S. Y. Jeong, R. W. Park, I. S. Kim, I. C. Kwon, *J. Control. Release* **2006**, *111*, 228–234.
- 23 K. Kim, S. Kwon, J. H. Park, H. Chung, S. Y. Jeong, I. C. Kwon, I. S. Kim, *Biomacromolecules* **2005**, *6*, 1154–1158.
- 24 J.S. Park, T. H. Han, K. Y. Lee, S. S. Han, J. J. Hwang, D. H. Moon, S. Y. Kim, Y. W. Cho, *J. Control. Release* **2006**, *115*, 37–45.
- 25 G. Saravanakumar, K. H. Min, D. S. Min, A. Y. Kim, C. M. Lee, Y. W. Cho, S. C. Lee, K. Kim, S. Y. Jeong, K. Park, J. H. Park, I. C. Kwon, *J. Control. Release* **2009**, *140*, 210–217.
- 26 S. J. Lee, H. Koo, D. E. Lee, S. Min, S. Lee, X. Chen, Y. Choi, J. F. Leary, K. Park, S. Y. Jeong, I. C. Kwon, K. Kim, K. Choi, *Biomaterials* **2011**, *32*, 4021–4029.
- 27 N. Duhem, J. Rolland, R. Riva, P. Guillet, J. M. Schumers, C. Jérôme, J. F. Gohy, V. Préat, *Int. J. Pharm.* **2012**, *423*, 452–460.
- 28 J. P. Quiñones, K. V. Gothelf, J. Kjems, A. M. H. Caballero, C. Schmidt, C. P. Covas, *Carbohydr. Polym.* **2012**, *88*, 1373–1377.
- 29 S. J. Lee, K. Park, Y. K. Oh, S. H. Kwon, S. Her, I. S. Kim, K. Choi, S. J. Lee, H. Kim, S. G. Lee, K. Kim, I. C. Kwon, *Biomaterials* **2009**, *30*, 2929–2939.
- 30 S. Park, S. J. Lee, H. Chung, S. Her, Y. Choi, K. Kim, K. Choi, I. C. Kwon, *Microsc. Res. Tech.* **2010**, *73*, 857–865.
- 31 J. Lee, C. Lee, T. H. Kim, E. S. Lee, B. S. Shin, S. C. Chi, E. S. Park, K. C. Lee, Y. S. Youn, *J. Control. Release* **2012**, *161*, 728–734.
- 32 J. Key, C. Cooper, A. Y. Kim, D. Dhawan, D. W. Knapp, K. Kim, J. H. Park, J. H. Park, K. Choi, I. C. Kwon, K. Park, J. F. Leary, *J. Control. Release* **2012**, *163*, 249–255.
- 33 F. Uchegbu, A. Siew, *J. Pharm. Sci.* **2013**, *102*, 305–310.
- 34 Y. Yang, J. Bugno, S. Hong, *Polym. Chem.* **2013**, *9*, 2651–2657.
- 35 C. Y. Chuang, T. M. Don, W. Y. Chiu, *J. Polym. Sci. Part A: Polym. Chem.* **2010**, *48*, 2377–2387.
- 36 C. Y. Chuang, T. M. Don, W. Y. Chiu, *J. Polym. Sci. Part A: Polym. Chem.* **2009**, *47*, 5126–5136.
- 37 S. Kwon, J. H. Park, H. Chung, I. C. Kwon, S. Y. Jeong, *Langmuir* **2003**, *19*, 10188–10193.
- 38 F. Huang, K. J. Shui, H. Y. Li, M. Y. Hu, G. H. Zhong, *Pestic. Biochem. Physiol.* **2011**, *99*, 16–24.